Detection of SARS-COVID-19 Based on CT Images Using Deep Learning-Based Hybrid Particle Swarm and Mayfly Optimization Algorithm

Manish K. Assudani* and Neeraj Sahu
Raisoni Centre for Research and Innovation, G. H. Raisoni University, Amravati, India
Email: mkasudani@gmail.com (M.K.A.), neeraj.sahu@ghru.edu.in (N.S.)

***Abstract*—More than 25 million people worldwide have contracted COVID-19 due to the SARS-COV-2 disease. Screening many suspected cases for quarantine and treatment is crucial to controlling the disease. Pathogenic laboratory testing is the gold standard but has a high false-negative rate, making alternate diagnostic procedures necessary to fight the disease. Based on COVID-19 radiographic changes in Computed Tomography (CT) scans, this research hypothesized that artificial intelligence (AI) approaches may extract particular graphical features and offer a clinical diagnosis before the pathogenic test, saving time for disease management. 1065 CT images of pathogen-confirmed COVID-19 and typical viral pneumonia patients were obtained. To develop the method, we proposed Deep Learning (DL)-based hybrid Particle Swarm Optimization and Mayfly Optimization (PSO-MFO) algorithm. PSO-MFO as a classifier to detect SARS-COVID-19. Internal validation yielded accuracy, specificity, and sensitivity. The external testing dataset has accuracy, specificity, and sensitivity. These findings show that AI can extract radiological features for COVID-19 diagnosis.**

***Index Terms*—COVID-19, Particle Swarm Optimization (PSO), Mayfly Optimization (MFO), CT scan**

I. Introduction

The WHO proclaimed the worldwide pandemic of the coronavirus illness of 2019 (COVID-19) in early March 2020. Internationally, a total of 659 million patients diagnosed, including 0.668 million fatalities, have been notified to WHO because of COVID-19 infection induced by SARS-CoV-2 as of December 11th, 2022 [1]. Nevertheless, these figures are rising and are anticipated to soar in the next months due to the virus's greater regenerative capacity. Consequently, it is crucial to stop the transmission of viruses, which can only be done by isolating and treating viral cases as soon as they are discovered.

In general, reverse transcriptase-polymerase chain reaction (RT-PCR), chest X-ray (CXR), and computed tomography (CT) are the three main screening techniques utilized for early detection of COVID-19 [2]. The conventional COVID-19 diagnostic RT-PCR technique finds viral RNA in oropharyngeal swabs or mucus, but it is labor-intensive, time-consuming, and requires specialized staff and materials. Rapid antigen testing, which provides a quicker and more inexpensive identification than PCR but has poor susceptibility to COVID-19, is an additional option to the RT-PCR test [3]. Radiographic tests have been discovered to be particularly beneficial in detecting and evaluating the COVID-19 disease process. The latest research investigations on the evaluation of COVID-19 by RT-PCR, CT, and CXR scans have been carried out by qualified radiologists. A case report highlighting the occurrence of a false negative result in the RT-PCR test for COVID-19. The study underscores the significance of utilizing chest CT imaging as a complementary diagnostic tool, particularly when clinical suspicion remains despite negative test outcomes. This emphasizes the potential limitations of relying solely on RT-PCR testing for accurate COVID-19 diagnosis and emphasizes the role of imaging techniques in enhancing diagnostic accuracy [4]. Nevertheless, due to its mobility and pricey installation, frequent use of lung CT is not practical due to the sudden increase of COVID-19 patients.

There is a requirement for technological solutions to identify and help in the diagnosis utilizing tried-and-true methods like deep learning (DL) and extraction of deep features. Artificial Intelligence (AI) based approaches have been effective in disease detection, and thus the number of COVID-19 cases globally has grown considerably. Convolutional neural network (CNN) models (ResNet50, Inception-v3, and Inception-ResNetV2) were used in a recent study [5] to identify COVID-19 infection among patients, with a high precision of 97.9%. Also employed in [6] have been several pre-trained DL models, which used two groups to reach 98.14% precision and 93.12% recall (COVID-19 vs. normal conditions).

Due to the precision and computation limits of the current testing approaches, it is essential to identify COVID-19 patients as soon as possible so that they may seek medical help. Studies have demonstrated that

Manuscript received May 7, 2023; revised July 10, 2023;; accepted September 2, 2023.
*Corresponding author

COVID-19 may be detected using radiological imaging such as X-ray or CT scans [7]. These studies have demonstrated the advantages of employing radiological imaging for COVID-19 detection. However, in this situation, medical professionals must read these photographs to recognize the patients. Machine Learning (ML) models may be used to enhance disease diagnosis using radiographic images, which can aid medical professionals by reducing variability and time required for diagnosis. Therefore, high-precision evaluation by ML models is necessary to urge regulators to adopt these methods and produce precise and rapid solutions [8].

The main contributions of this paper are as follows:

- To create a new hybrid PSO-MFO algorithm, the original MFO and PSO algorithms are updated and given the idea of the group's median position. The group's newly introduced median position allows each swarm-mayfly to use more of the information from the group to determine its behavior, ensuring the group's diversity and helping to maintain a balance between the stages of exploration and exploitation as well as the algorithm's search effectiveness.
- To save time on disease management by utilizing DL to extract certain graphical elements and provide medical assessment before the pathogenic test.
- To assess the diagnostic efficacy of a proposed hybrid PSO-MFO based on DL while screening for COVID-19 utilizing CT images.
- 1065 CT scans of COVID-19 individuals with a verified pathogen and instances of previously identified typical viral pneumonia have been enlisted to test this idea. The outcomes show that it is possible to extract radiographic visual characteristics for COVID-19 diagnosis using the DL and proposed PSO-MFO approach as a proof-of-concept.

The rest of the paper has been organized: Section II describes related research on ML and DL with optimization for the detection and diagnosis of COVID-19. Section III provides a novel framework called Deep Learning (DL)-based hybrid Particle Swarm Optimization and Mayfly Optimization (PSO-MFO) algorithm to detect COVID-19. Results and discussion have been given in Section IV. Finally, the conclusion, limitations, and scope for further research have been shown in Section V.

II. Related Works on ML and DL for the Detection of COVID-19

Recently, a variety of AI-based techniques for COVID-19 identification utilizing chest x-ray and CT images have been developed by researchers. Although the use of DL techniques led to more favorable statistical findings, the model development stage of these studies still must be improved to achieve a treatable condition for categorization and segmentation. For illustration, according to the initial research project by Wang *et al*. [9], DL models effectively identified COVID-19 symptoms in CXR scans. For the COVID-19 class, models effectively predict outcomes with an accuracy of 80%. However, lowering false negatives is crucial for creating a reliable detection mechanism.

The COVID-SDNet approach, which tends to reduce false negatives and categorize COVID-19 into several intensity tags as light, medium, serious, and normal, was proposed by the author in the study work [10]. By removing portions outside chest regions from the raw picture that did not include lung segmentation, models created the publicly available COVIDGR-1.0 dataset and introduced segmentation-based scaling. Additionally, ResNet50 performance was enhanced using reconfiguration and advancements of CXR scans based on the GAN model, which increased accuracy to 98% overall and 87% in severe and moderate instances.

In the study, Shamsi suggested a transfer learning-based deep uncertainty-aware model for CT and CXR analysis [11]. To recognize COVID-19, the suggested study extracts features using four deep learning approaches: InceptionResNetV2, ResNet50, VGG16, and DenseNet121. According to the statistical study, SVM and neural networks have better accuracy and sensitivity for the two-class issue, ranging from 88% to 97%. A classification model with two stages of classification was proposed by Wang *et al*. in their research work [3]. The Discrimination-DL stage extracted lung characteristics, and the Localization-DL stage localized features in the left and right lung regions. This network exhibited 93.01% efficiency for the localization network and 98.71% efficiency for Discrimination-DL.

In research [12], the author created a graph-based method for identifying COVID-19 diseases with no monitoring needed. This quasi-supervised learning system uses faux tagging to deal with numerous unlabeled examples. Results were better at recognition using attention maps than the supervised framework. The ConvNet model is built using DL and fuzzy logic models in reference research [13]. When a multi-layer perceptron is given features for classification that are retrieved using a hybrid of deep and fuzzy logic techniques and reach 81% accuracy, the model learns better.

Some study models have been created employing the traditional CXR modality and CT, ultrasound, or heterogeneous information combining CXR and CT images. However, relative to the CXR modality, employing CT scans in practical testing restricts mobility and is more costly. To diagnose COVID-19 in this situation, Owais *et al*. [14] suggested a light DL ensemble network by fusing "FCNet, ShuffleNet, and MobileNet". Radiologists can identify infections using model-focused localization and engagement map display. However, a group of CXR and CT records with mean F1-scores of 95.94% and 94.60% are used to evaluate the model.

A dual-sampling attention network was used in a different model [15] that was put out for utilizing 3D-CT volumes to diagnose community-acquired influenza. Double sampling fixes the class imbalance issue, and the attention mechanism more accurately detects disease in CT data, exceeding the most advanced UNet model. The study used fourfold cross-validation to analyze a sample of 2186 CT images with the tags COVID-19/NORMAL. F1-score and precision of the quantitative tests were 82.5%

and 88.1%, respectively. The bulk of previous research use CXR and CT methods in combination with transfer learning models to diagnose COVID-19.

For the detection of COVID-19 in chest CT scans, another coherent conceptual framework [16] named Joint segmentation and classification (JCS) was developed. JCS combines segmentation and classification to detect COVID-19 illness in CT images. A sizable database of 150,104 CT images from 345 normal CT scans and 450 COVID-19 patients was gathered for the proposed study. Reported CT scans from 3795 patients are part of the COVID-CS database for virus identification. JCS has a classification sensitivity and specificity of 94.8% and 92.9%, respectively, compared to an illness segmentation dice score of 79.1%.

Particle swarm algorithm, bacterial foraging algorithm, moth-killing algorithm, Mayfly algorithm, beetle search algorithm, and cuckoo search algorithm are just a few examples of the numerous swarm intelligence optimization algorithms that researchers and academics have progressively implemented into the detection of COVID-19 [17, 18]. Additionally, while these approaches have their benefits, there are also some drawbacks, particularly in the case of large-scale and complicated issues. These drawbacks include extensive computation times, a tendency to enter the local optimum, and premature convergence easily.

The chest X-rays of the lungs are a diagnostic tool for COVID-19 that is extensively used; however, the interpretation of them can be problematic due to the presence of minor alterations in the lungs induced by the virus, which was apparent in the images. This can make it difficult to determine whether or not the individual has COVID-19. This is the situation despite the fact that pulmonary radiography is utilized rather frequently. This article presents a CNN model that can be used for identifying categories of data obtained from pulmonary radiography. The model was developed by the authors in [19] of this article. A series of radio-graphs of the lungs taken from patients who had been diagnosed with COVID-19 were used to validate and improve the model that was proposed. According to the findings of the research, the CNN model performed noticeably better than the conventional approaches did when it came to the categorization of the data. This was demonstrated by the fact that the CNN model outperformed them. The predicted model was found to be 96.2% accurate, while its sensitivity was found to be 96.8%. Both of these figures are very impressive. It was shown that it has the potential to be used for purposes other than classifying the data connected with the existence of COVID-19. This potential was proved by the findings of the study. Additionally, radiologists might utilise it as a tool to assist them in the interpretation of the lungs radiography that has been taken.

This paper presents a high-density feature representation model for multi-domain study of human health issues to address feature representation and classification limitations. The model generates comprehensive health feature vectors from patient-specific information from multi-domain sources such blood reports, ECGs, EEGs, social media posts, and physiological indicators. These components increase feature density, which aids disease classification. These features estimate high-variance feature sets in Bee Colony Optimization Models.

This paper employs a new hybrid PSO-MFO algorithm, where the original MFO and PSO algorithm is updated and given the idea of the group's center position. The group's newly introduced center position allows each swarm and mayfly to use more of the information from the group to determine its behavior, ensuring the group's diversity and helping to maintain the algorithm's search effectiveness and avoiding early convergence.

III. Deep Learning (DL)-Based Hybrid Particle Swarm Optimization and Mayfly Optimization (PSO-MFO) Algorithm

In this part, the basic stages of the proposed DL-based PSO-MFO are covered in more detail in the following subsections to categorize patients showing COVID-19 and non-COVID-19 diseases using CT image datasets. The trial pictures obtained from the COVID-CT image collection have been explained in the first part [20]. The pre-processing that has been performed on these CT images to normalize their input to the DL-based feature extraction is described in the second part. Methods for extracting the features using DL have been described in the third part. The proposed hybrid PSO-MFO classifier utilized to conduct the tests is finally presented in the fourth part. The suggested technique's steps are seen in Fig. 1.

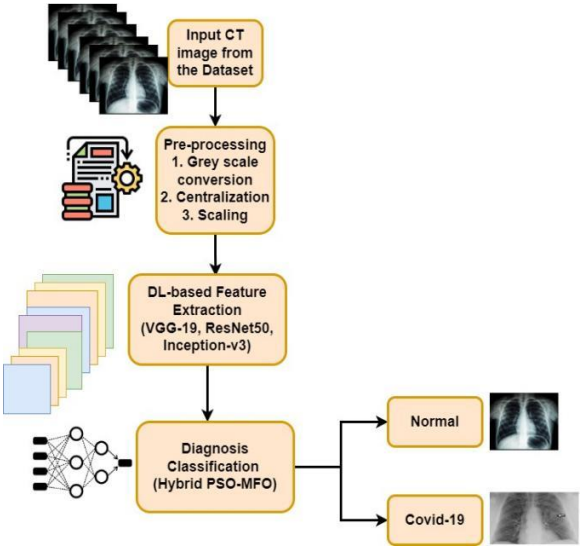

Fig. 1. Structure of the proposed DL-based hybrid PSO-MFO.

A. Dataset

Prospectively, the CT scans of 1065 patients have been gathered, 505 of whom had normal viral pneumonia, and 510 came from three hospitals where SARS COV-2 had been positively identified by nucleic acid testing. In addition, 50 more COVID individuals have been added whose initial diagnosis has been made despite the first two nucleic acid tests being negative. Before transmitting

any CT pictures for examination, they have all been verified again. Each collaborating institute's institutional review board has approved this study. The trials in the study have been carried out to categorize patients into COVID-19 and non-COVID-19 groups.

B. Pre-Processing

Neither the CT digitization procedure nor the assessment methods unify the images obtained from the dataset. A pre-processing step has been used to normalize the CT pictures utilized in this procedure. Three further stages make up this phase. First, it is noted that color-scale patterns rather than grayscale are visible in the pictures from the COVID CT collection. Due to the possibility of the classifier being influenced by certain patterns, this prohibits us from employing them. To get over this issue and maintain the technique's simplicity, grayscale conversion has been done, where all images (from the COVID CT imaging database) have been changed to grayscale. The images vary in breadth and height. As a result, scaling has been used to preserve the CT scans' structural features. It was started by determining the greatest axis and making a rectangle picture whose height and breadth corresponded to its dimensions. The source image is now placed in the center of the new square image. All images have been scaled down to 224×224 pixels. This size was chosen since it was appropriate for additional DL processing but did not reduce the quality of the gathered images.

C. DL-Based Feature Extraction

This stage aims to gather a standardized analysis of the lungs seen in the CT images; these data have been utilized in the categorization step. The difficult job of extracting characteristics from a picture necessitates a high degree of skill, which requires considerable effort and time. The answers might not be generally valid for other scenarios because the task is difficult and the features gained are particular to the issue. Extraction of features has become viable with the advancement of deep Neural Network (NN) models.

Fig. 2 depicts the DL-based feature extraction framework. CNN's layers serve as feature representations. The lower levels learn basic characteristics like boundaries and outlines, color and pattern are extracted by the intermediate layers, and the entity in the image is learned by the deeper layers. These models furthermore have a fully linked layer that serves as a classifier. In this study, the method for extracting features is known as "DL-based features." It entails taking a standard CNN and deleting its fully connected layer to produce a feature representation as the system's output. As a result, CNN becomes an automatic feature extractor. Three network designs have been chosen for the tests: VGG19, Resnet50, and Inception-v3.

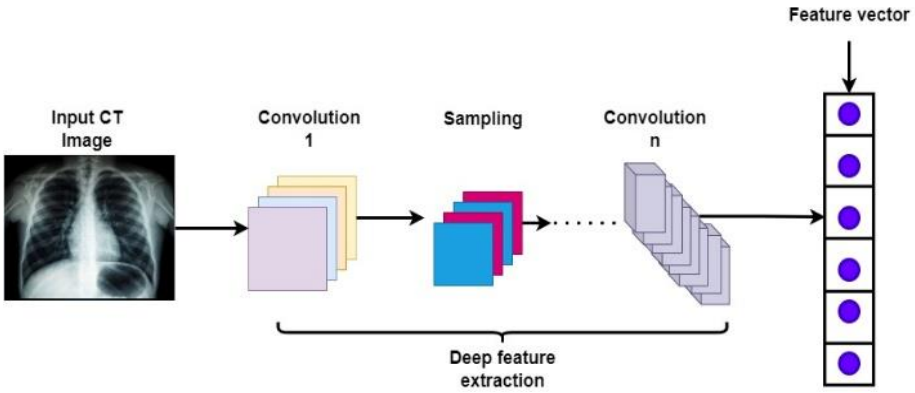

Fig. 2. DL-based feature extraction framework.

D. Diagnosis Classification Using Hybrid PSO-MFO

1) PSO algorithm

Natural groups' flocking and cooperative activity served as the inspiration for the PSO algorithm, an evolutionary approach [17]. By gradually altering particle placements and velocities following the group's and particle's flying events, it finds the optimal solution, directing the particles towards the position of g_{best} and p_{best} in the next iterations. g_{best} is the highest population fitness value that any particle has ever attained, whereas p_{best} is the highest particle fitness value that has ever been attained. Compared to other optimization approaches, PSO may produce a superior solution in less duration with more efficient and steady convergence characteristics. Additionally, there are fewer settings to tweak, and it is more effective at sustaining the swarm's variety since every particle uses data from the most effective component (the g_{best} particle) to better itself.

A four-position vector has been constructed to indicate a PSO particle, with each vector component standing for particular key parameters. Each characteristic needs a search area, essentially the range of possible values for the parameter's highest and lowest values. A distinct threshold of between four and nine has been established for the maximum depth. The minimum offspring weights have been specified as real numbers ranging from two to six. Lastly, consistent limits between zero and one have been established for the remaining parameters. A fitness function has been necessary to enable the PSO algorithm to develop. Using the outcomes of the XGBoost system, which worked on the verification subgroup following the chosen variables, each particle's fitness has been assessed.

2) MFO algorithm

As a brand-new kind of smart optimization method, the Mayfly algorithm has great optimization and study

potential [21]. Additionally, it draws inspiration from mayfly social conduct, particularly the breeding process. It is presumed that the most suited mayfly will survive after emerging from the egg as an individual. Additionally, each mayfly's location inside the search area suggests a potential answer to the issue. The algorithm's basic tenets of operation are as follows: Mayflies have been divided into two groups randomly to reflect male and female swarms. Each mayfly has been arbitrarily positioned as a possible alternative y=(y_1, y_2, ⋯, y_e) expressed by a e-dimensional matrix and its competence has been assessed using a specified objective function $O(y)$. Additionally, the variation in the mayfly's location is what is meant by the definition of its speed, S=(S_1, S_2, ⋯, S_e). Each mayfly's flight path reflects the constant relationship between the individual and the notion of the cooperative movement. Eventually, every mayfly will continually modify its path to reach its ideal position thus far (p_{best}) and the global best thus far attained by the entire group (g_{best}).

3) Hybrid PSO-MFO

The fundamental mayfly optimization technique is more accurate and faster at convergence than conventional PSO approaches. However, other regional optimum and delay phenomena might occur throughout the solution search phase. This study proposes a hybrid PSO-MFO to enhance the algorithm's overall search effectiveness and precision. The mayfly algorithm's gravitational factor is comparable to PSO's gravitational factor and aids in striking a balance between extraction and discovery. Therefore, a non-linear gravitational factor has been employed in this paper to gradually reduce the gravitational coefficient at the start of the iteration, allowing for improved discovery, the avoidance of hitting the regional optimum, and a quick convergence rate. The gravitational factor is increased and lowered later in the cycle, which enhances the search for the best solution. A non-linear gravitational factor can also help strike a good balance between discovery and exploitation. The non-linear gravitational factor has the following formula:

$$gf(t) = 0.5\,\text{sqrt}\left(1 + \frac{t}{t_{\max}}(t + t_{\max})^2\right) \tag{1}$$

where t and $t_{\max}$ are the number of iterations and the maximum number of iterations in the PSO-MFO algorithm. Upon introducing $gf(t)$, the speed or velocity of a male swarm-mayfly is given as

$$s_{k,l}^{t+1} = gf(t)s_{k,l}^{t} + b_1 \exp(-\alpha c_p^2)\left(p_{\text{best}_{k,l}} - y_{k,l}^{t}\right) + b_2 \exp(-\alpha c_g^2)\left(g_{\text{best}_{k,l}} - y_{k,l}^{t}\right) \tag{2}$$

where $s_{k,l}^{t=1}$ and $s_{k,l}^{t}$ are the speed at time t+1 and t, respectively, in measurement k and period l. $gf(t)$ is the non-linear gravitational factor. b_1 and b_2 are the desirability coefficients of swarm-mayfly. The perceptibility factor is denoted as α. c_p^2 is the proximity between the present location and p_{best}. c_g^2 is the proximity between the present location and g_{best}. $y_{k,l}^{t}$ is the location of the male swarm-mayfly in measurement k and period l at time t. The speed updating process of the male swarm-mayfly has been given as:

$$s_{k,l}^{t=1} = \begin{cases} gf(t)s_{k,l}^{t} + b_2 \exp(-\alpha c_{\text{fm}}^2)\left(z_{k,l}^{t} - y_{k,l}^{t}\right), \\ \qquad \text{for } O(z_k) > O(y_k) \\ gf(t)s_{k,l}^{t} + \text{rw} \cdot c, \text{ for } O(z_k) \le O(y_k) \end{cases} \tag{3}$$

where c_{fm}^2 is the proximity between female and male swarm-mayfly. $z_{k,l}^{t}$ is the location of the female swarm-mayfly during measurement k and period l at time t. rw is the randomized walking factor of swarm-mayfly. c is the arbitrary value lying between −1 and +1. $O(z_k)$ and $O(y_k)$ are the objective function corresponding to female and male swarm-mayfly during measurement k.

Given the fundamentals of the PSO and MFO algorithms, it is easy to see how the hybrid PSO-MFO algorithm utilizes the benefits of the PSO, Genetic Algorithm (GA), and MFO algorithm, which could be seen as an upgrade of the PSO and MFO algorithms. In addition, the MFO and PSO algorithms are comparable in modifying the swarm-mayfly's speed and location. As a result, the suggested hybrid PSO-MFO algorithm's adaptation of the swarm-mayfly mobility is based on the cooperative exchange of similar science knowledge to provide an evolutionary benefit. Personalized recollection and general intelligence are the key topics covered in this information. The optimal answer allows individual memory to take the best location for each participant and social intelligence to choose the best position for the whole group. Hence, in the proposed hybrid PSO-MFO algorithm, attaining p_{best} is based on the MFO algorithm, and obtaining g_{best} is based on the PSO algorithm.

It can be inferred from the speed update equation for the male swarm-mayfly algorithm that the revised speed is composed of three components. The first component is the speed $y_{k,l}^{t}$ of the swarm-mayfly in the initial state; the second component is the location (p_{best}–$y_{k,l}^{t}$) between the present position of the swarm-mayfly and the participant's ideal location; this component is referred to as the "perspective" component because it shows that the individual knows about their own; The third component, known as the "society" component, measures how far the mayfly's actual location (g_{best}–$y_{k,l}^{t}$) is from the swarm's best location. This proximity measures how well the mayfly cooperates with the details given by the swarm to reach the optimal position. Hence, it is apparent that the swarm-mayfly's motion process is impacted by its group as a whole and by the ideal location in which it resides.

However, there is no other method for the mayflies to share data; only through g_{best} and p_{best} information shared and transmitted throughout the swarms. As a result, the mayflies have a solitary source of knowledge and little knowledge transfer. It is also simple to eliminate the population's variety when moving. In addition, early convergence occurs due to the swarm-mayfly's rapid clustering, which frequently traps the cluster in a regional optimum. Therefore, it is simple to miss some critical data if just the best member in the swarm is highlighted throughout the process of group optimization.

Additionally, relying exclusively on the data provided by g_{best} and p_{best} is insufficient. Whether a group is excellent or evil, they may all provide knowledge to the movement. The data of other participants should also be taken into account and utilized in the discovery process in addition to g_{best} and p_{best}. Additionally, the group's search space should not be constrained to the region described by the last two criteria.

The variety of the population, which is a key characteristic, is strongly correlated with the lack of convergence efficiency, the slow rate of later development, and the quick convergence in the evolutionary process. Cluster heterogeneity is, therefore, essential to the algorithm's overall convergence. Furthermore, there is an uncertainty that the heterogeneity of the group might be expanded by expanding the exchange of group information and individual experience knowledge. Based on the above, this study adds a group's median location based on g_{best} and p_{best}. Since excessive numbers often influence the average, the median and average are frequently employed in statistics to show the general average level.

However, the allocation of individuals within the group is somewhat dispersed in the swarm-based algorithm's early stage of geographical discovery, and there are a few individuals whose placements are quite bad. As a result, using the median to represent the group's location as a whole may not be correct. The suggested hybrid PSO-MFO, which arranges all the swarm-mayfly members based on their objective function value $O(y)$ and $O(z)$ introduces the idea of the median location of the groups depending on the median concept and uses the median location of the swarm-mayfly as the group's median location. The median location of the swarm-mayfly is given as:

$$\text{ML} = \begin{cases} \frac{y_{m/2}+y_{(m/2)+1}}{2}, \text{ if } m \text{ is even} \\ \frac{y_{(m/2)+1}}{2}, \text{ if } m \text{ is odd} \end{cases} \quad (4)$$

where ML is the median location of the swarm-mayfly. m is the number of groups. The ML value is the average location of the group and has been incorporated into the updated speed equation of the male swarm-mayfly is given as:

$$s_{k,l}^{t+1} = gf(t)s_{k,l}^{t} + b_1 \exp(-\alpha c_p^2)\left(p_{\text{best}_{k,l}} - y_{k,l}^{t}\right) + b_2 \exp(-\alpha c_g^2)\left(g_{\text{best}_{k,l}} - y_{k,l}^{t}\right) + b_3 \exp(-\alpha c_{\text{ml}}^2)\left(\text{ML}_{k,l} - y_{k,l}^{t}\right) \quad (5)$$

where b_1, b_2, and b_3 are the desirability coefficients of swarm-mayfly. The perceptibility factor is denoted as α. c_{ml}^2 is the proximity between the present location and the median location $\text{ML}_{k,l}$.

The optimal hybrid PSO-MFO settings for the model validation phase have been identified after this classification for the diagnosis of COVID-19. A test dataset has been utilized to determine the method's resilience, and verification parameters have been obtained.

IV. Results and Discussion

The Python library has been employed to accomplish the suggested technique. With TensorFlow-GPU serving as the back-end, it has largely utilized the Keras deep learning library. The PC utilized for these tests has a Windows 10 operating system, an Intel Core i7-7700 K 4.20 GHz CPU, 16 GB of RAM, and an Nvidia GeForce GTX 1080-Ti graphics card.

It originally included 260 patients, from which the group contained 179 cases of normal viral pneumonia detected before the COVID-19 epidemic, to create a hybrid PSO-MFO algorithm for detecting viral pneumonia images. In the group, these individuals have been referred to as COVID-19 negative. The remaining 80 cases came from the health centers where SARS-COV-2 nucleic acid screening, also known as COVID-19 positive, has been verified.

Fig. 3 depicts the loss curves and accuracy of the training phase using the proposed hybrid PSO-MFO algorithm for the classification of COVID-19 infection from CT images. After falling, the loss trajectory and accuracy tend to remain steady, proving that the training process conforms. The model has been created to modify the hyper factor during training, and the verified accuracy has been assessed every 500 steps. The loss and accuracy curves both tended to be steady after 9000 epochs.

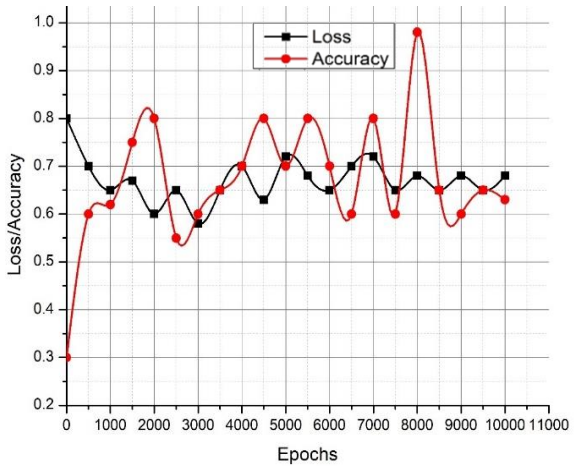

Fig. 3. Loss curves and accuracy of the training phase using the proposed hybrid PSO-MFO algorithm for classifying COVID-19 infection from CT images.

Fig. 4 shows the characteristic plot for the detection of COVID-19 using a DL-based hybrid PSO-MFO algorithm with (a) internal and (b) external validation. Two physicians reviewed the images and then drew 1065 sample images (739 for COVID-19 negative results and 326 for COVID-19 positive results) for evaluation. These images have been split into a training dataset and validation data at random. With an early learning rate of 0.005, the model training has been repeated 10,000 times. To build the model, 310 images—155 from the COVID-19 negative and 155 from the COVID-19 positive—were collected. To assess the sustainability and generality of the proposed approach, 280 images (215-COVID-19 negative images and 65-COVID-19 positive images) have been gathered from centers 2 and 3 for external validation,

and 445 images (355-COVID-19 negative images and 90-COVID-19 positive images). The area under ROC is 0.94 and 0.82 for internal and external validation, respectively.

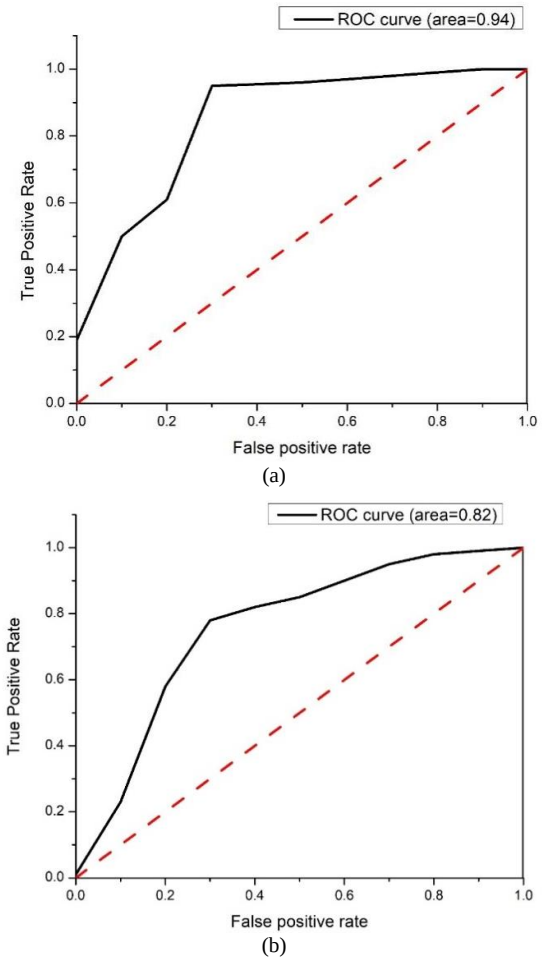

Fig. 4. Characteristic plot for the detection of COVID-19 using DL (inception)-based hybrid PSO-MFO algorithm with (a) internal validation and (b) external validation.

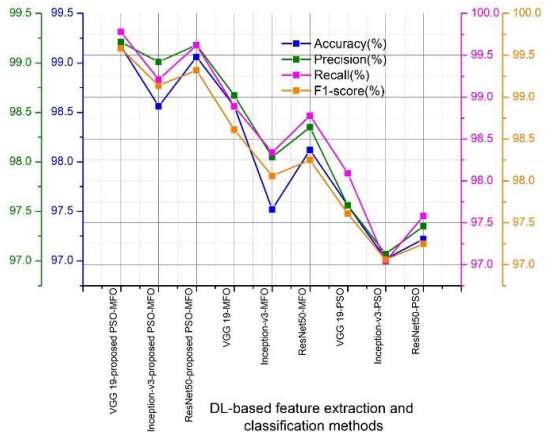

Fig. 5. Comparison of DL-based feature extraction and classification methods for the detection of COVID-19.

Fig. 5 compares DL-based feature extraction and classification methods for detecting COVID-19. The subsequent stage is to implement the algorithms to the testing dataset, compute the metrics to assess their performance, and show why the PSO-MFO is superior to the other optimization techniques once all the characteristics for the network models have been improved using PSO, MFO, and the proposed hybrid PSO-MFO. A study of the validation measures for different combinations is shown in Fig. 5. Additionally, the suggested hybrid PSO-MFO was the only one that could achieve 99.5% in two different types of architecture for the measure of Precision and Recall (VGG19 and ResNet50). For the metric of F1-score, providing synchronization between precision and recall, the proposed algorithm reached 99% in all three architectures (VGG19, Inception-v3, and ResNet50). The F1-Score variance in these two topologies exhibits a similar pattern, particularly in VGG19, where there was just a 0.22% standard deviation. It, therefore, emphasizes how reliable the hybrid PSO-MFO was in optimizing successfully and swiftly and generating encouraging validation measures.

Table I gives the performance comparison of the proposed DL-based hybrid PSO-MFO algorithm (internal and external validation) and trained radiotherapists to detect COVID-19. Two expert radiotherapists will evaluate the 745 images for a forecast. The accuracy of radiotherapist 1 was 74.5% with a precision of 75.1% and an F1-score of 70.5%; the accuracy of radiotherapist 2 was 73.9% with a precision of 75.1% and an F1-score of 70.7%. (As observed in Table I). These findings show that radiotherapists found it challenging to predict COVID-19 using eye scanning, highlighting another benefit of the approach suggested in this paper.

Table II shows the detection of COVID-19 using the proposed hybrid PSO-MFO versus bacterial pneumonia.

The proposed technique has been validated using the hybrid PSO-MFO on CT scans of patients suffering from bacterial pneumonia. The whole batch of images was fed into the model, and the classification outcome was gathered. As seen in Table II, the model identified 91.65% of the patients as not having COVID-19. It demonstrates that the model successfully distinguishes individuals with bacterial pneumonia from COVID-19. Although the model sometimes misdiagnoses patients, it is important to note that the diagnostic choice is supported by several laboratory and clinical tests and that this model assists the radiotherapist. A disagreement in the proper categorization results from pneumonia's respiratory patterns being identical to those of COVID-19.

TABLE I: PERFORMANCE COMPARISON OF THE PROPOSED DL-BASED HYBRID PSO-MFO ALGORITHM (INTERNAL AND EXTERNAL VALIDATION) AND TRAINED RADIOLOGISTS FOR THE DETECTION OF COVID-19

Parameters (%)	Internal validation	External validation (ROI)	External validation (patients)	Radio therapist 1	Radio therapist 2
Accuracy	98.3	88.4	90.6	74.5	73.9
Precision	99.1	89.2	89.5	75.1	75.1
Recall	99.2	88.9	91.2	75.8	75.7
F1-score	99.3	89.3	91.5	70.5	70.7

TABLE II: DETECTION USING PROPOSED HYBRID PSO-MFO VERSUS BACTERIAL PNEUMONIA

Detection	Number	Percentage
False detection of COVID-19	219	8.35%
True detection of non-COVID-19	2401	91.65%
Total detections made	2620	100%

TABLE III: DETECTION USING PROPOSED HYBRID PSO-MFO VERSUS VIRAL PNEUMONIA

Detection	Number	Percentage
False detection of COVID-19	100	6.06%
True detection of non-COVID-19	1550	93.93%
Total detections made	1650	100%

Table III shows the detection of COVID-19 using the proposed hybrid PSO-MFO versus viral pneumonia. In this study, the proposed technique employing hybrid PSO-MFO in CT scans of patients with viral pneumonia has been validated, much as the testing is done with bacterial pneumonia. The outcomes are displayed in Table III. It can be observed that the model was successful in separating viral pneumonia patterns from COVID-19-caused illness. There has been a mistake in the classification of some tests, much like there is with bacteria. It is important to note that this tool is meant to be used by professionals as a checking and support tool rather than to treat patients. Similar to the previous test in Table II, it should be kept in mind that other pneumonia causes significant respiratory dysfunction, which causes disagreement for the classifier. The model classified 93.93% as non-COVID-19 patients.

V. CONCLUSION AND FUTURE WORK

The COVID-19 pandemic has had a global influence. There have been several techniques created to help frontline workers. The current study provided a completely automated technique for extracting feature representations from CT images using CNN-based DL techniques. It also suggested utilizing PSO-MFO optimization to classify if the images show COVID-19 or normal lungs. 1065 CT images of pathogen-confirmed COVID-19 and typical viral pneumonia patients were obtained. A pre-processing procedure was required to normalize the test findings since we used non-standard datasets. The characteristics of the images were then automatically extracted using a CNN-based features extraction technique. For classification, a novel hybrid PSO-MFO algorithm has been employed. The original MFO and PSO algorithm is modified and provided with a notion of the group's median location in the hybrid PSO-MFO. Each swarm-mayfly can now use more of the information from the group to determine its behavior, thanks to the newly introduced median position for the group. This ensures the group's diversity and aids in maintaining a balance between the stages of exploration and exploitation as well as the effectiveness of the search algorithm. The suggested hybrid PSO-MFO was the only one that could achieve 99.5% in two different types of architecture for the measure of Precision and Recall (VGG19 and ResNet50). For the metric of F1-score, providing synchronization between precision and recall, the proposed algorithm reached 99% in all three architectures (VGG19, Inception-v3, and ResNet50). In the future, integrating the hierarchical CT image characteristics to those of additional parameters, such as genetic, epidemiological, and clinical data, to do multi-modeling analysis can aid in improved diagnosis.

CONFLICT OF INTEREST

The authors declare no conflict of interest

AUTHOR CONTRIBUTION

Both authors contributed the work equally.

REFERENCES

[1] A. L. García-Basteiro, C. Chaccour, C. Guinovart *et al.*, "Monitoring the COVID-19 epidemic in the context of widespread local transmission," *The Lancet Respiratory Medicine*, vol. 8, no. 5, pp. pp. 440–442, 2020.

[2] D. A. Altantawy and S. S. Kishk, "Equilibrium-based COVID-19 diagnosis from routine blood tests: A sparse deep convolutional model," *Expert Systems with Applications*, vol. 213, #118935, 2023.

[3] Z. Wang, Y. Xiao, Y. Li *et al.*, "Automatically discriminating and localizing COVID-19 from community-acquired pneumonia on chest X-rays," *Pattern Recognition*, vol. 110, #107613, 2021.

[4] H. Feng, Y. Liu, M. Lv, and J. Zhong, "A case report of COVID-19 with false negative RT-PCR test: necessity of chest CT," *Japanese Journal of Radiology*, vol. 38, no. 5, pp. 409–410, 2020.

[5] A. Narin, C. Kaya, and Z. Pamuk, "Automatic detection of coronavirus disease (Covid-19) using x-ray images and deep convolutional neural networks," *Pattern Analysis and Applications*, vol. 24, no. 3, pp. 1207–1220, 2021.

[6] I. D. Apostolopoulos and T. A. Mpesiana, "Covid-19: automatic detection from x-ray images utilizing transfer learning with convolutional neural networks," *Physical and Engineering Sciences in Medicine*, vol.43, no. 2, pp. 635–640, 2020.

[7] Z. Zhang, X. Li, W. Zhang *et al.*, "Clinical features and treatment of 2019-nCov pneumonia patients in Wuhan: report of a couple cases," *Virologica Sinica*, vol. 35, no. 3, pp. 330–336, 2020.

[8] L. Gaur, U. Bhatia, N. Z. Jhanjhi *et al.*, "Medical image-based detection of COVID-19 using deep convolution neural networks," *Multimedia Systems*, vol. 29, no. 3, pp. 1729–1738, 2021.

[9] L. Wang, Z. Q. Lin, and A. Wong, "COVID-net: A tailored deep convolutional neural network design for detection of COVID-19 cases from chest x-ray images," *Scientific Reports*, vol. 10, no. 1, # 19549, 2020.

[10] S. Tabik, A. Gómez-Ríos, J. Martín-Rodríguez *et al.*, "COVIDGR dataset and COVID-SDNet methodology for predicting COVID-19 based on chest X-ray images," *IEEE Journal of Biomedical and Health Informatics*, vol. 24, no. 12, pp. 3595–3605, 2020.

[11] A. Shamsi, H. Asgharnezhad, S. Jokandan *et al.*, "An uncertainty-aware transfer learning-based framework for COVID-19 diagnosis," *IEEE Trans. on Neural Networks and Learning Systems*, vol. 32, no. 4, pp. 1408–1417, 2021.

[12] A. Aviles-Rivero, P. Sellars, C. Schönlieb *et al.*, "GraphXCOVID: explainable deep graph diffusion pseudo-labelling for identifying COVID-19 on chest X-rays," *Pattern Recognition*, vol. 122, #108274, 2022.

[13] C. Ieracitano, N. Mammone, M. Versaci *et al.*, "A fuzzy-enhanced deep learning approach for early detection of Covid-19 pneumonia from portable chest X-ray images," *Neurocomputing*, vol. 481, pp. 202–215, 2022.

[14] M. Owais, H. Yoon, T. Mahmood *et al.*, "Light-weighted ensemble network with multilevel activation visualization for robust diagnosis of COVID19 pneumonia from large-scale chest radiographic database," *Applied Soft Computing*, vol. 108, #107490, 2021.

[15] X. Ouyang, J. Huo, L. Xia *et al.*, "Dual-sampling attention network for diagnosis of COVID-19 from community acquired pneumonia," *IEEE Trans. on Medical Imaging*, vol. 39, no. 8, pp. 2595–2605, 2020.

[16] Y. Wu, S. Gao, J. Mei *et al.*, "Jcs: An explainable covid-19 diagnosis system by joint classification and segmentation," *IEEE Trans. on Image Processing*, vol. 30, no. 7, pp. 3113–3126, 2021.

[17] D. Júnior, L. da Cruz, J. Diniz *et al.*, "Automatic method for classifying COVID-19 patients based on chest X-ray images, using deep features and PSO-optimized XGBoost," *Expert Systems with Applications*, vol. 183, #115452, 2021.

[18] A. Farki, Z. Salekshahrezaee, A. Tofigh *et al.*, "COVID-19 diagnosis using capsule network and fuzzy -means and mayfly

optimization algorithm", *BioMed Research International*, vol. 2021, #2295920, 2021.
[19] S. Shivadekar, B. Kataria , S. Hundekari *et al.*, "Deep Learning Based Image Classification of Lungs Radiography for Detecting COVID-19 using a Deep CNN and ResNet 50," *International Journal of Intelligent Systems and Applications in Engineering*, vol. 11, no. 1s, pp. 241–250, 2023.
[20] https://www.eibir.org/covid-19-imaging-datasets/
[21] G. Lei, X. Chang, Y. Tianhang, and W. Tuerxun, "An improved mayfly optimization algorithm based on median position and its application in the optimization of PID parameters of hydro-turbine governor," *IEEE Access*, vol. 10, pp. 36335–36349, 2022.

Manish K. Assudani received his master's of computer science and engineering from the RTM Nagpur University, Maharashtra, India in 2010. He is currently as assistant professor in the Department of Computer Science & Engineering, Nagpur, Maharashtra, India. At present he is a research scholar at G.H.Raisoni, University, Amravati. His research interests include data mining, deep learning, artificial intelligence, machine learning, cyber and security.

Neeraj Sahu received the Ph.D. degree in computer science and engineering from the Singhania University, Rajasthan, India in 2014. He is currently as assistant professor in G.H.Raisoni University, Amravati, Maharashtra, India. His research interests include data mining, e-commerce, recognition, cyber and security. He is visited Singapore in April 2012 for paper presentation. He worked as project fellow in Maulana Azad National Institute of technology (MANIT Bhopal) on research project. He received his Post Doctoral Fellowship (PDF) from Indian Agricultural Statistics Research Institute New Delhi on research project. He worked as Assistant professor for 3 years in Maulana Azad National Institute of Technology (MANIT Bhopal). Supervised eight PhD Scholar as Supervisor three is awarded and five under process near submission of thesis. He is Published and Granted many Patents. He is Published many SCI/Scopus/Web of Science Article and Conferences proceeding. He is Published many books and book Chapters.